

INTERNATIONAL JOURNAL ON SMART SENSING AND INTELLIGENT SYSTEMS SPECIAL ISSUE, SEPTEMBER 2017



DESIGN AND IMPLEMENTATION OF DUAL-BAND CIRCULARLY POLARIZED ANTENNAS USING STACKED PATCHES

S Sankaranarayanan¹, M Anto Bennet^{1*}, B. Deepa², A. Banu², S. Gayathri²

¹Faculty of Electronics and Communication Engineering, Vel Tech, Chennai, India.

²UG Student of Vel Tech, Chennai, India.

Email: bennetmab@gmail.com

Submitted: May 27, 2017 Accepted: June 15, 2017 Published: Sep 1, 2017

Abstract- Single and Dual feed Antennas with dual frequencies have been demonstrated. Varactor diodes are used for independent tuning. The PIFA (Planar Inverted F-Antenna) has two frequencies from 0.7 to 1.1 GHz and from 1.7 to 2.3GHz. Impedance match of about -10dB an isolation greater than 13dB is obtained. The single feed antenna can be tuned from 1.2 to 1.6GHz and 1.6 to 2.3 GHz. The antenna volumes are 63x100x3.15 mm³ with relative permittivity is 3.55 substrates. The efficiency varies from 25% to 50% over tuning range. The application areas are in 4G wireless systems.

Index terms: Planar inverted F-antenna (PIFA), Voltage Standing Wave Ratio(VSWR)

I. INTRODUCTION

An antenna (or aerial) is an electrical device which converts electric power into radio waves, and vice versa. It is usually used with a radio transmitter or radio receiver. In transmission, a radio transmitter supplies an electric current oscillating at radio frequency (i.e. a high frequency alternating current (ac)) to the antenna's terminals, and the antenna radiates the energy from the current as electromagnetic waves (radio waves). In reception, an antenna intercepts some of the power of an electromagnetic wave in order to produce a tiny voltage at its terminals, which is applied to a receiver to be amplified. Antennas are essential components of all equipment that uses radio. They are used in systems such as radio broadcasting, broadcast television, two-way radio, communications receiver radar, cell phones, and satellite communications, as well as other devices such as garage door openers, wireless microphones, Bluetooth-enabled devices, wireless computer networks, baby monitors, and RFID tags on merchandise. Micro strip Antenna is a kind of antenna used to process ultra-high frequency signals 300MHz-3GHz (3000MHz). It is made by etching the antenna pattern into metal trace. This etching is bonded to a layer of insulating material plastic, glass or crystals. It consists of a metallic patch on one side of a dielectric substrate and ground plane on the other side of the substrate. The patch acts approximately as a resonant cavity (short circuit walls on top and bottom, open circuit walls on the sides). If the antenna is excited at a resonant frequency, a strong field is set up inside the cavity, and a strong current on the surface of the patch. This produces significant radiation.

Two dual band antennas are designed with single feed and dual feed. Co-axial feed is given to the antenna and the material used in the substrate is ROGERS R04003. Biasing is done by altering the values using HFSS software in order to achieve tuning. Dual band antenna is a high frequency antenna consisting of Lower band from 0.7-1.1GHz and higher band from 1.7-2.3GHz. The main advantage is that tuning can be achieved by using varactor diodes.

II. Literature Survey

The operation frequencies are the most crowded bands in wireless communications since they are unlicensed by any international agreement or government authority. Therefore, efficiently utilizing the limited spectrum in such bands is very crucial and indispensable. A new design approach for a Microstrip Patch Antenna to achieve reconfigurable dual band operation with (1.45 to 1.63GHz) and capacitance range is from 0.31 to 0.74 pF. Antenna prototype operating in

2-4.5GHz [1]. The author [2] had proposed antenna dimension of about $24(0.44)*22(0.403)\text{mm}^2$ resonant frequencies at 2 and 3.3GHz. The author [3] had proposed that -10dB wide impedance bandwidth from 4.2-7.3GHz. Author had proposed a dual polarized compact microstrip antenna using multilayer electromagnetic bandgap with conducting layer for GSM & WiMAX application. The author [4] had proposed that a compact size probe feed microstrip antenna operating frequencies at 4 GHz and increased gain of 7dB is achieved. The author [5] had proposed that design of dual band 3.65GHz(802.11Y) and 5.8GHz(802.11a) antenna using U-slot. The author [6] had proposed that UWB antenna has overall size of $26 \times 30 \times 1.6\text{mm}^3$ and works at 3-11GHz with $\text{VSWR} < 2$. The author [7] had proposed that antenna works about 3.4GHz good performance with -10dB return loss bandwidth of % and bandwidth of 4.2% with circularly polarized gain of about 10.97dB. The author [8] had proposed that a single feed planar inverted F-Antenna (PIFA) with independent frequency tunability is 700-970MHz and 1600-2200MHz using two varactor diodes. Generally, an Omni directional pattern is provided to communicate in all directions. The most suitable pattern can be configured on demand with the pattern reconfigurable antenna. Different arrangements of parasitic elements with different lengths around the active element yield different radiation patterns. This offers a simple and flexible method for beam forming. The afore mentioned pattern-reconfigurable antennas are available only in single band, and the sizes are comparatively large. Therefore, a compact dual-band pattern-reconfigurable antenna is introduced here [9,10].

III. Proposed System

The proposed system includes Dual-feed Planar inverted F-antenna (PIFA) antennas with coaxial feed by using HFSS Ansoft. Directivity, return loss, antenna gain and radiation pattern of the dual band antenna is obtained. Two antennas with single feed and dual feed are optimized and their parameters are obtained. Dual band antenna gives better performance with efficiency from 25% to 50% while tuning. The range of the return loss is below -10dB for single feed, -13dB for double feed and VSWR is less than 3dB. Radiation pattern, Gain, Return loss, Directivity and VSWR of the proposed antenna is obtained. Since tuning cannot be done in varactor diode, values are changed till constant biasing is achieved. The substrate used is ROGERS R04003, which is the material that acts as an insulator. Since tuning cannot be done manually, biasing is done till a constant value is achieved.

IV. Explanation

4.1. Dual Band Antenna

A dual-band feeding antenna that is less sensitive is required to maintain good impedance in different surrounding Matching conditions caused by the combinations of the reflection states of the sidewalls. It is hard to use an impedance-matching network to satisfy the various radiating conditions at two frequencies. In this paper, the lower resonant frequency of the dual-band Feeding antenna is designed to be excited by couplings, which have relatively broad bandwidths at dual bands than by the conventional direct feeding method. Thus, acceptable return losses at the desired frequencies can be achieved for various switch states. The proposed dual-band feeding antenna is shown in Fig.1. The front part directly excites the higher frequency radiation while the back part combined with the former by coupling effects resonates at the lower frequency. The suitable amount of coupling can be obtained by adjusting w_t , h and g_2 .

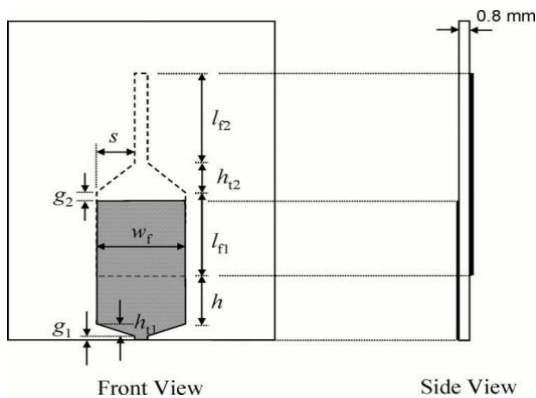


Fig.1 Typical dual band feeding antenna

4.2. Single Feed Dual Band Antenna

Fig. 2 presents the single-feed dual contiguous-band antenna. The antenna is printed on the $63 \times 100 \times 3.15 \text{mm}^3$ substrate with permittivity= 3.55 similar to the dual feed dual-band antenna, and same varactor diodes (Skyworks SMV1232-040LF) are used tune the antenna. Ten-k Ω resistors are used to bias the varactor diodes at points $B1$ and $B2$. The same substrate and biasing pad configuration as the dual-feed dual-band antenna are used. Similar to the dual-feed dual-band antenna, the single feed antenna has two branches: 1) one resonating at the low-band and 2) the other resonating at the high-band.

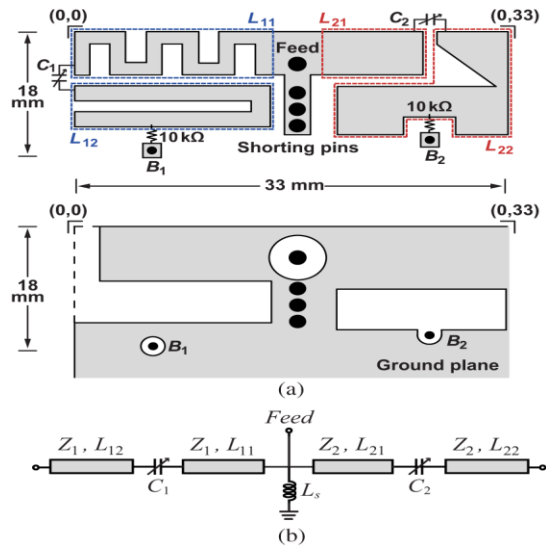


Fig.2.Single feed Dual Band Antenna Geometry

- (a) Top view and bottom view. All dimensions are in mm.
- (b) Transmission line model

The transmission-line model for the antenna is presented in Fig. 2 (b). The varactor diode capacitances C_1 and C_2 are used to tune the two different antenna resonant frequencies. The lower resonance frequency can be tuned from 1.2 to 1.6 GHz and the higher resonance frequency can be tuned from 1.6 to 2.3 GHz. These frequencies do not coincide with the traditional LB, MB, and HB regions for CA standards, and were chosen to demonstrate a dual-tuned antenna with near contiguous tuning, covering a 1.2–2.3-GHz range and fabrication shown in fig 3.

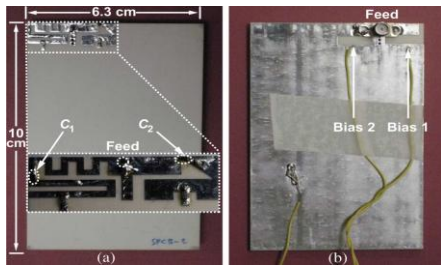


Fig 3.Fabricated single-feed dual contiguous band-antenna

- (a) top plate
- (b) ground plate

4.3. Dual Feed Dual Band Antenna

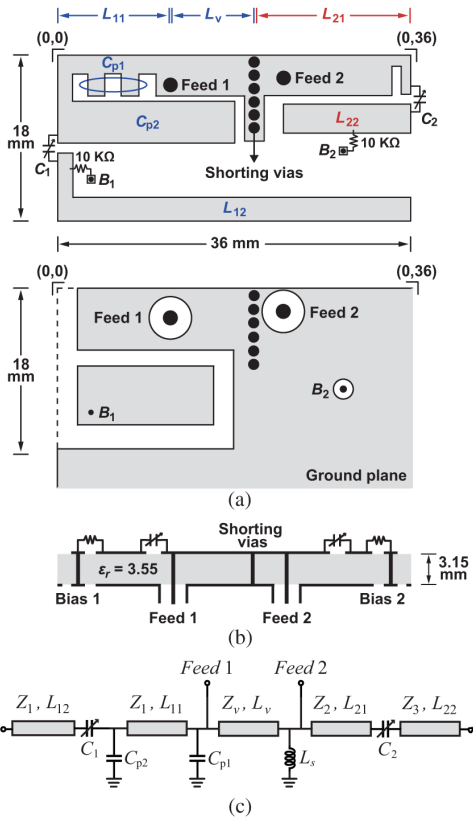


Fig.4. Dual-feed dual-band antenna geometry

- (a) Top metal plate and ground plate
- (b) Cross section. All dimensions are in mm.
- (c) Transmission-line model

The dual-feed dual-band antenna is shown in Fig. 4. The antenna resonance frequency is controlled using two varactor diodes (Skyworks SMV1232-040LF, $C_{tot} = 0.8\text{--}3.8$ pF, $Bias = 0\text{--}20$ V). The antenna is printed on a $63 \times 100 \times 3.15$ mm³ substrate stack which is formed by two 1.524 mm thick Rogers RO4003 C substrates (permittivity= 3.55, $\tan \delta = 0.0027$ at 2.5 GHz) joined by a 0.101-mm Rogers RO4450B bond ply (permittivity= 3.54, $\tan \delta = 0.004$ at 10 GHz). In several other implementations, the antenna is made of sheet copper and suspended in air or printed on a low permittivity plastic carrier. The choice of the substrate here is only for research/demonstration purposes since it is low cost and provides mechanical robustness for soldering. The PIFA has two feeds that are used for low-band (feed 1) and high-band (feed 2)

operations. All frequencies above 1.7 GHz are referred to as high-band (that is the mid-band and high-band are lumped together into one band). Shorting vias of the LB and high-band (HB) PIFAs are combined together and placed between the feeds. The inductance of the six shorting vias is simulated using ANSYS HFSS to be 0.17 nH, and results in a high isolation between the LB and HB PIFA arms. This makes it possible to independently tune the two resonance frequencies. Fig. 4 (c) presents the transmission-line model, and is based on the tunable PIFA model described in Section II. Two tunable PIFAs are merged together at their short circuit sections and the inductive effects of the shorting vias are captured as L_{sin} in the transmission-line model. The LB and HB resonances are controlled by varactor diodes C_1 and C_2 , respectively. To reduce the antenna size, short sections of open-ended transmission lines are added to the LB PIFA. The tuning characteristics were simulated with surface impedance boundary conditions at the tuning device ports using ANSYS HFSS. The low-band operation, using feed 1, covers the 0.7–1.1 GHz band, whereas the high-band operation, using feed 2, covers the 1.7–2.3 GHz band and fabrication shown in fig 5.

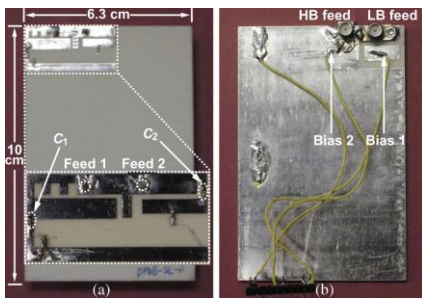


Fig.5 Fabricated dual-feed dual-band antenna for CA

(a) top plate (b) ground plate.

V. Experimental Results

Design procedure of tunable dual band antenna

The substrate is created as shown in fig 6. The substrate used in the proposed antenna is ROGERS R04003 and the permittivity of the antenna is 3.55 substrates. The volume of the antenna is $63 \times 100 \times 3.15 \text{ mm}^3$. The patch of the antenna is created on the substrate. This describes the front portion of the antenna before the substrate. The patch and ground of the antenna is created along with the shorting pins. 6 shorting pins are created as shown in the fig 8. The patch of the antenna after is separated after the creation of substrate. The separated slot of the antenna

Design and implementation of dual-band circularly polarized antennas using stacked

is shown in fig 9. The overall patch of the antenna without the slot appears to be as shown in fig.10. After the creation of the substrate, the ground for tuneable dual band antenna is created as shown below.11. The full view of the created ground of the proposed antenna is shown in fig.12. The front view of the complete antenna with the ground and the patch together is created as shown below13. A radiation box for the proposed antenna is created in order to obtain the radiation pattern of the antenna shown in fig 14. Finally, after feeding the antenna appears to be as shown in fig 15. The simulated return losses are shown in Fig.16. Generally, the return loss of the antenna should be designed so as to have less than -10dB. The proposed antenna has both lower frequency and higher frequency bands. In the lower frequency band, the simulated -15.25dB bandwidth is from 0.7 to 1.1 GHz,. In the higher band, the simulated bandwidth is -13.48dB between 1.7 and 2.3 GHz. A slight frequency shift may occur in the higher frequency region which might be caused by feeding method.

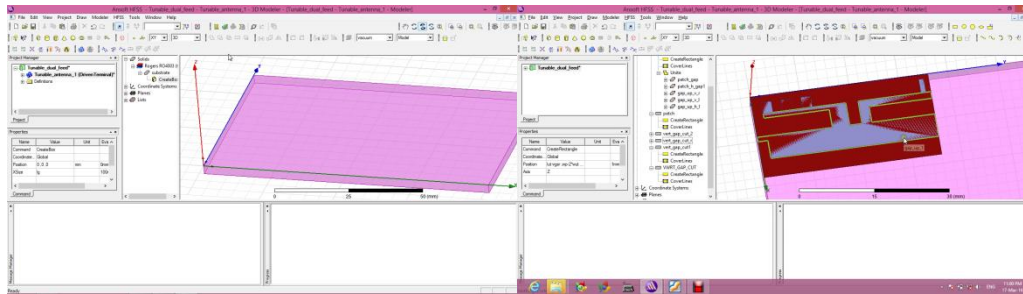


Fig.6. Substrate of the antenna

Fig.7.Creation of patch before the substrate

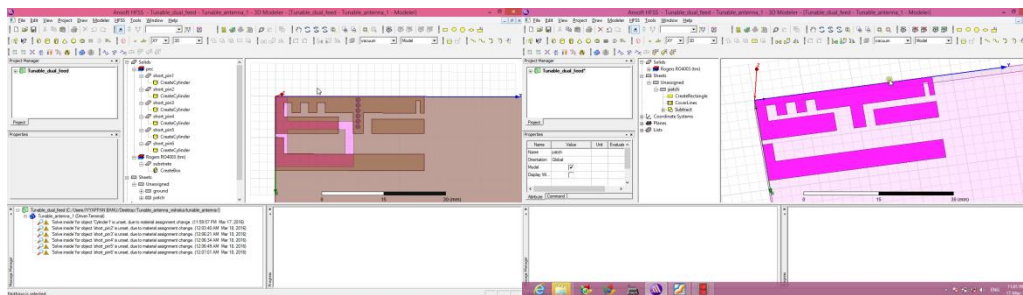


Fig 8.Ground and patch of the antenna along with shorting pins

Fig.9.Patch of the antenna after the substrate has been isolated

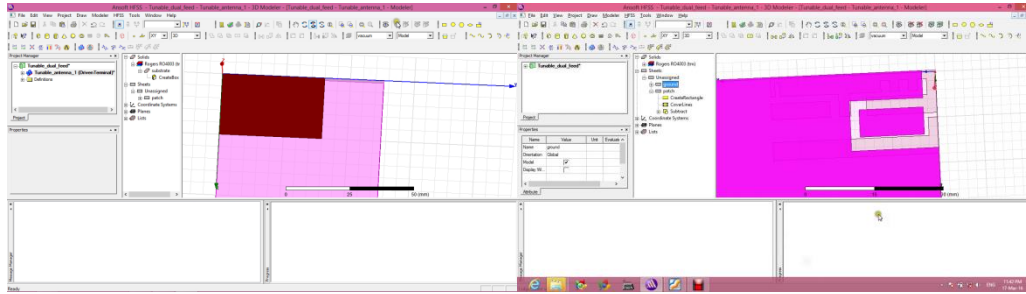


Fig.10. Patch of the antenna without slot

Fig 11.Ground of the antenna after the substrate

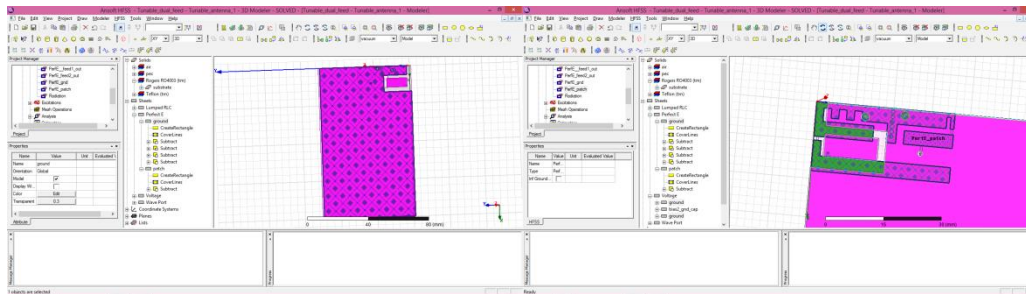


Fig.12. Full view of the ground of the antenna

Fig 13.Complete front view of the antenna

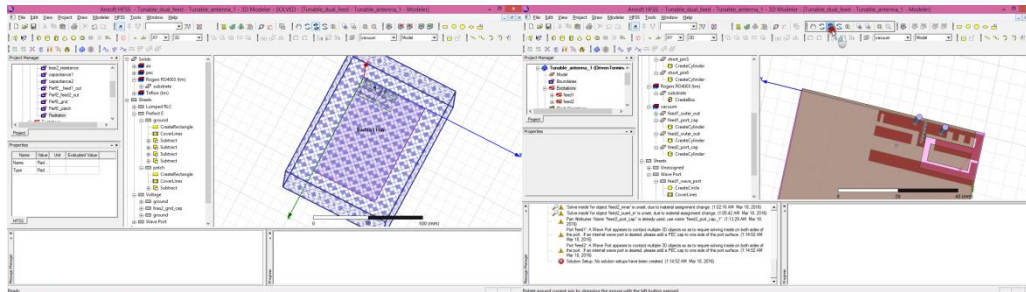


Fig 14.Radiation box of the antenna

Fig 15.Proposed antenna after feeding

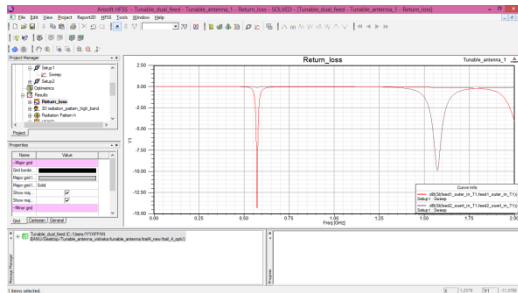


Fig 16.Return loss of tunable dual band antenna

5.1.Radiation Pattern

The radiation patterns of the antenna were measured using a Satimo SG32 spherical near-field chamber. The measured and simulated radiation efficiency is plotted in fig 17. The efficiency increases as the antenna is tuned to higher frequencies. This is because the antenna radiation Q decreases with frequency and the varactor diode Q increases as the capacitance decreases (i.e., with frequency). Radiation patterns are mostly isotropic for all of the tuning cases and as expected from PIFAs. The radiation pattern of the higher and lower band antenna is as shown below 18.

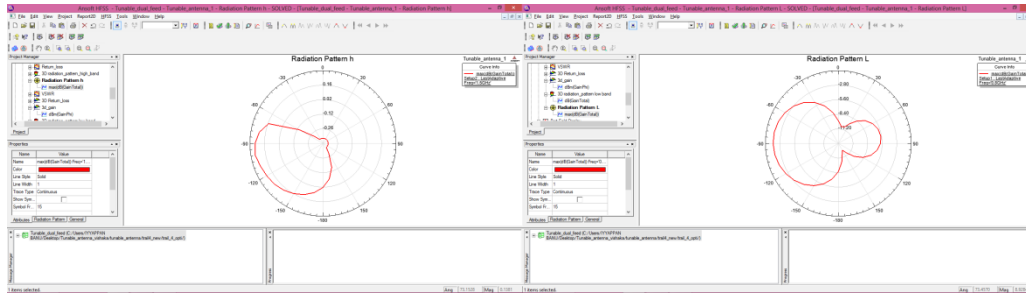


Fig.17.Radiation pattern of high band antenna

Fig.18.Radiation pattern of low band antenna

5.2.VSWR

The Voltage Standing Wave Ratio of the antenna is usually less than 3dB and less than 1dB for a best antenna. The proposed antenna is so designed to have +0.57dB as shown in fig.19.

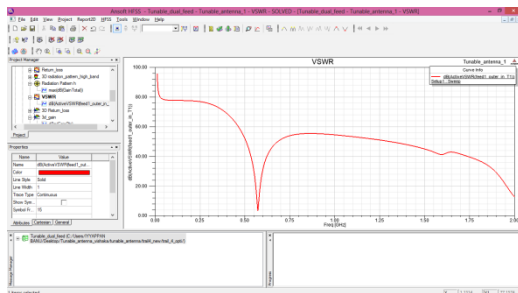


Fig.19.VSWR of the tunable dual band antenna

D plots of the parameters of tunable dual band antenna-Gain

The gain is obtained as 2.4dBi for tunable dual band antenna as shown in fig.20. And their radiation pattern shown in fig 21,22 and 23.

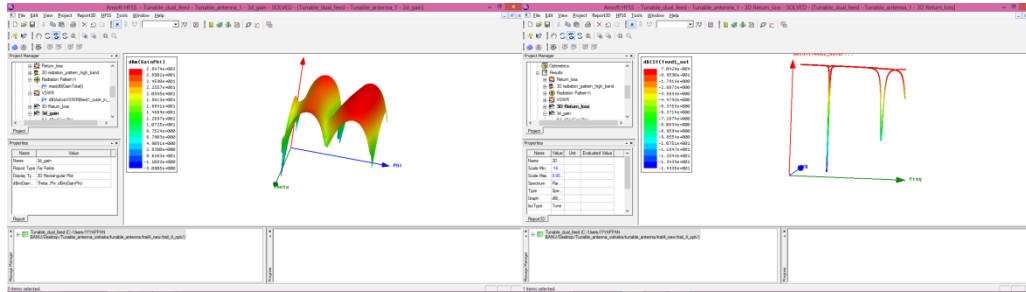


Fig.20. Gain of the antenna in 3d plot

Fig.21. Return loss in 3d plot

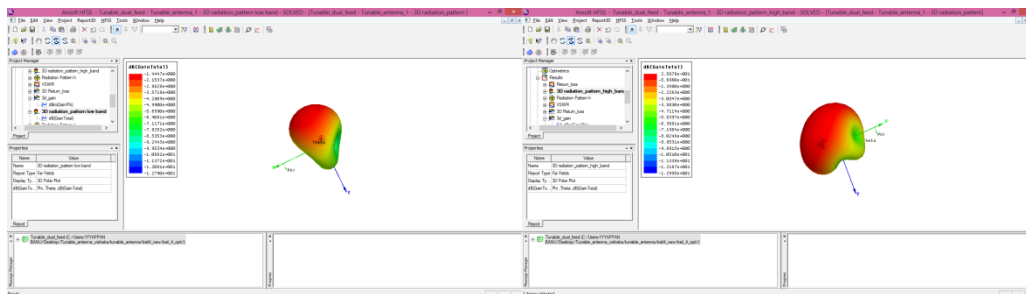


Fig.22. Radiation pattern of Lower Band Antenna

VI. Conclusion

A dual-feed dual-band PIFA covering the 0.7–1.1 GHz and 1.7–2.3 GHz bands has been demonstrated using varactor diodes. There exists a high isolation between the bands; hence the two resonance frequencies can be tuned independently without affecting each other. Additionally, a single-feed antenna with two independently tunable resonant frequencies is demonstrated at 1.1–2.3 GHz using varactor diodes. The efficiencies of the both antennas can be increased significantly by using RF MEMS varactors. In practice, and when these antennas are used in cell phones and with hand and body loading effects, the antennas will become more wideband and less efficient, and a lot of additional effort is needed to build a true working dual-band antenna on actual platform. The goal of this work is to show that dual-tuned PIFAs are a promising candidate for increasing the performance of communications systems using the 3GPP LTE CA standard.

REFERENCES

- [1] Aizat Azmi, Ahmad Amsyar Azman, Sallehuddin Ibrahim, and Mohd Amri Md Yunus, "Techniques In Advancing The Capabilities Of Various Nitrate Detection Methods: A Review", *International Journal on Smart Sensing and Intelligent Systems.*, VOL. 10, NO. 2, June 2017, pp. 223-261.
- [2] Tsugunosuke Sakai, Haruya Tamaki, Yosuke Ota, Ryohei Egusa, Shigenori Inagaki, Fusako Kusunoki, Masanori Sugimoto, Hiroshi Mizoguchi, "Eda-Based Estimation Of Visual Attention By Observation Of Eye Blink Frequency", *International Journal on Smart Sensing and Intelligent Systems.*, VOL. 10, NO. 2, June 2017, pp. 296-307.
- [3] Ismail Ben Abdallah, Yassine Bouteraa, and Chokri Rekik , "Design And Development Of 3d Printed Myoelectric Robotic Exoskeleton For Hand Rehabilitation", *International Journal on Smart Sensing and Intelligent Systems.*, VOL. 10, NO. 2, June 2017, pp. 341-366.
- [4] S. H. Teay, C. Batunlu and A. Albarbar, "Smart Sensing System For Enhanceing The Reliability Of Power Electronic Devices Used In Wind Turbines", *International Journal on Smart Sensing and Intelligent Systems.*, VOL. 10, NO. 2, June 2017, pp. 407- 424
- [5] SCihan Gercek, Djilali Kourtiche, Mustapha Nadi, Isabelle Magne, Pierre Schmitt, Martine Souques and Patrice Roth, "An In Vitro Cost-Effective Test Bench For Active Cardiac Implants, Reproducing Human Exposure To Electric Fields 50/60 Hz", *International Journal on Smart Sensing and Intelligent Systems.*, VOL. 10, NO. 1, March 2017, pp. 1- 17
- [6] P. Visconti, P. Primiceri, R. de Fazio and A. Lay Ekuakille, "A Solar-Powered White Led-Based Uv-Vis Spectrophotometric System Managed By Pc For Air Pollution Detection In Faraway And Unfriendly Locations", *International Journal on Smart Sensing and Intelligent Systems.*, VOL. 10, NO. 1, March 2017, pp. 18- 49
- [7] Samarendra Nath Sur, Rabindranath Bera and Bansibadan Maji, "Feedback Equalizer For Vehicular Channel", *International Journal on Smart Sensing and Intelligent Systems.*, VOL. 10, NO. 1, March 2017, pp. 50- 68
- [8] Yen-Hong A. Chen, Kai-Jan Lin and Yu-Chu M. Li, "Assessment To Effectiveness Of The New Early Streamer Emission Lightning Protection System", *International Journal on Smart Sensing and Intelligent Systems.*, VOL. 10, NO. 1, March 2017, pp. 108- 123
- [9] Iman Heidarpour Shahrezaei, Morteza Kazerooni and Mohsen Fallah, "A Total Quality Assessment Solution For Synthetic Aperture Radar Nlfm Waveform Generation And Evaluation

In A Complex Random Media”, International Journal on Smart Sensing and Intelligent Systems., VOL. 10, NO. 1, March 2017, pp. 174- 198

[10] P. Visconti ,R.Ferri, M.Pucciarelli and E.Venere, “Development And Characterization Of A Solar-Based Energy Harvesting And Power Management System For A Wsn Node Applied To Optimized Goods Transport And Storage”, International Journal on Smart Sensing and Intelligent Systems., VOL. 9, NO. 4, December 2016 , pp. 1637- 1667

[11] YoumeiSong,Jianbo Li, Chenglong Li, Fushu Wang, “Social Popularity Based Routing In Delay Tolerant Networks”, International Journal on Smart Sensing and Intelligent Systems., VOL. 9, NO. 4, December 2016 , pp. 1687- 1709

[12] Seifeddine Ben Warrad and OlfaBoubaker, “Full Order Unknown Inputs Observer For Multiple Time-Delay Systems”, International Journal on Smart Sensing and Intelligent Systems., VOL. 9, NO. 4, December 2016 , pp. 1750- 1775

[13] Rajesh, M., and J. M. Gnanasekar. "Path observation-based physical routing protocol for wireless ad hoc networks." International Journal of Wireless and Mobile Computing 11.3 (2016): 244-257.

[14]. Rajesh, M., and J. M. Gnanasekar. "Congestion control in heterogeneous wireless ad hoc network using FRCC." Australian Journal of Basic and Applied Sciences 9.7 (2015): 698-702.

[15]. Rajesh, M., and J. M. Gnanasekar. "GCCover Heterogeneous Wireless Ad hoc Networks." Journal of Chemical and Pharmaceutical Sciences (2015): 195-200.

[16]. Rajesh, M., and J. M. Gnanasekar. "CONGESTION CONTROL USING AODV PROTOCOL SCHEME FOR WIRELESS AD-HOC NETWORK." Advances in Computer Science and Engineering 16.1/2 (2016): 19.

[17]. Rajesh, M., and J. M. Gnanasekar. "An optimized congestion control and error management system for OCCEM." International Journal of Advanced Research in IT and Engineering 4.4 (2015): 1-10.

[18]. Rajesh, M., and J. M. Gnanasekar. "Constructing Well-Organized Wireless Sensor Networks with Low-Level Identification." World Engineering & Applied Sciences Journal 7.1 (2016).

[19] A. Almomani, B. B. Gupta, S. Atawneh, A. Meulenberg, and E. Almomani, "A Survey of Phishing Email Filtering Techniques," in IEEE Communications Surveys & Tutorials, vol. 15, pp.2070-2090, 2013.

- [20] S. S. Tseng, K. Y. Chen, T. J. Lee, and I. F. Weng., "Automatic content generation for anti-phishing education game," in IEEE International Conference on Electrical and Control Engineering, pp.6390-6394, 2011.
- [21] F. Frattolillo, "Watermarking Protocol for Web Context," in IEEE Transactions on Information Forensics and Security, vol.2, no.3, sept, pp.350-363, 2007.
- [4] P. Sun, and H. Lu, "An efficient web page watermarking Scheme," in IEEE, pp.163-167, 2009.
- [22] H. Wang and C. Liao, "Compressed-Domain Fragile Watermarking Scheme for Distinguishing Tampered Image Content or Watermark," in IEEE, pp.480-484, 2009.
- [23] A .P. Singh, V. Kumar, S. S. Senger, and M. Wairiya, "Detection and Prevention of Phishing Attack using Dynamic Watermarking," in International Conference on Advances in Information Technology and Mobile Communication, vol. 147, pp 132-137, 2011.